Available online at www.sciencedirect.com
ScienceDirect
Polymer 48 (2007) 2526–2530
polymer
www.elsevier.com/locate/polymer

Polymer Communication

# Heterogeneity of a vulcanized rubber by the formation of ZnS clusters

Hidehiko Dohi [a], Shin Horiuchi [b,*]

[a] SRI Research & Development Ltd., 2-1-1 Tsutsui-cho, Chuo-ku, Kobe 651-0071, Japan
[b] Nanotechnology Research Institute, National Institute of Advanced Industrial Science and Technology, 1-1-1 Higashi, No. 5, Tsukuba, Ibaraki 305-8565, Japan

Received 8 December 2006; received in revised form 26 February 2007; accepted 1 March 2007
Available online 6 March 2007

**Abstract**

We investigated vulcanized rubber structures by energy-filtering transmission electron microscopy (EFTEM) and by high-angle annular dark field scanning transmission electron microscopy (HAADF-STEM). Both techniques revealed that numerous particles with the diameter of about 20 nm, which could not be observed by conventional TEM, were distributed in the rubber matrix. Further examination based on electron energy-loss spectroscopy (EELS) and energy-dispersive X-ray (EDX) analysis indicated that those particles are composed of ZnS clusters with the sizes of approximately 3–5 nm, which are produced as a by-product in the vulcanization. We believe that the formation of ZnS clusters in a rubber network is one of the origins of rubber heterogeneities.


*Keywords:* Vulcanization; Rubber; Heterogeneity

## 1. Introduction

Sulfur vulcanization is a key technology in the rubber industry which produces a wide variety of rubber materials. The process converts raw unsaturated polymers into their cross-linked forms through complicated chemical reactions in a mixture containing sulfur ($S_8$), accelerator (Acc) and activator. Although sulfur vulcanization has been employed as a large-scale industrial process for a long time and there have been numerous studies on their reaction mechanism and network structures, a thorough understanding of the processes and structures continue to be challenging [1].

The network structures have been known to greatly influence the elasticity and the ultimate properties of rubbers. If vulcanized rubbers could be formed into homogeneous three-dimensional structures at molecular level, their ultimate properties would be considerably higher than is presently achieved [2]. Therefore, the presence of inhomogeneity in rubber networks has been discussed theoretically [3,4] and experimentally [5–11] for a long time in terms of the heterogeneities of crosslink densities, entanglements and the network topologies. Heterogeneities of polymer networks have been investigated in gel materials by light and neutron scattering which showed the presence of concentration heterogeneities at submicrometer scales [12,13]. Heterogeneity of vulcanized rubber networks has been investigated by NMR techniques, which suggested the existence of domains of widely different molecular mobilities [11]. However, much difficulty is encountered in analyzing the uniformity of the sulfur networks owing to a number of reasons: (a) insolubility of cross-linked rubbers, (b) variety of chemical reactions that simultaneously take place within the polymers and at the surfaces of inorganic fillers, and (c) complicated heterogeneous structures.

Here we have employed two electron microscopic techniques for the investigation of heterogeneity of a vulcanized rubber. These are energy-filtering transmission electron microscopy (EFTEM) and high-angle annular dark field scanning transmission electron microscopy (HAADF-STEM). EFTEM enables us to create images with inelastically

* Corresponding author. Tel.: +81 29 861 6281; fax: +81 29 861 4773.
*E-mail addresses:* h-dohi.az@srigroup.co.jp (H. Dohi), s.horiuchi@aist.go.jp (S. Horiuchi).

0032-3861/$ - see front matter © 2007 Elsevier Ltd. All rights reserved.
doi:10.1016/j.polymer.2007.03.004

scattered electrons at given energy-loss levels, of which technique is called as "electron spectroscopic imaging" (ESI). Moreover, it enables us to perform electron energy-loss spectroscopy (EELS), which provides information on chemical compositions of local nano-sized areas in a specimen [14]. The latter is HAADF-STEM; it provides high-resolution imaging with contrast generated by differences in atomic number ($Z$) by collecting elastically scattered electrons scattered at higher angles than those scattered by the Bragg reflections [15]. Thus, this technique is powerful for observing objects including elements with high atomic numbers in polymers with minimum electron beam damage to specimens [16]. Introducing these two techniques, we performed elemental and chemical analyses of a vulcanized rubber structure.

## 2. Experimental

All the materials used in this study were commercial products and used "as received": an emulsion-type SBR was supplied by Zeon Corp. (Japan) with a grade name SBR1502. Sulfur ($S_8$) in 200-mesh powdery form was supplied by Tsurumi Chem. Co., Ltd. (Japan). ZnO in standard grade with the average particle size of 270 nm was supplied by Mitsui Mining & Smelting Co., Ltd. (Japan). Stearic acid (StAc) and *N-tert*-butyl-2-benzothiazolyl-sulfenamide (TBBS) used as an accelerator were supplied by NOF Corp. (Japan) and by Ouchi Shinko Chem. Ind. Co. (Japan), respectively. The rubber mixtures were compounded in an 8-in open roll mixer. The recipe of rubber mixtures was styrene-butadiene rubber (SBR), $S_8$, TBBS used as Acc, ZnO and StAc at 100/1.5/1.5/3/2 in weight. The open roll was cooled by circulating water at a temperature of 50 °C. Mixing was carried out for 10 min. Then, the compounded mixtures were thermally treated at 170 °C for 10 min in a hot press machine for vulcanization. Thin sections of the samples (about 100 nm thick) were prepared by cryo-ultramicrotomy at −60 °C and collected on a 600-mesh copper grid for EFTEM and STEM analyses.

A LEO922 in-column type energy-filtering transmission electron microscope with a $LaB_6$ cathode and equipped with an Omega-type energy filter was used at an accelerating voltage of 200 keV. All the observations were carried out cryogenically at 120 K using a Gatan 613-DH single tilt liquid nitrogen cooling holder to minimize the radiation damage to the specimens. For the analyses of sulfur and zinc elemental distributions by high-resolution elemental mapping and quantitative EELS analysis, we employed Image-EELS technique. The details of this technique were described in our previous papers [17,18]. First, a set of energy-filtered images was recorded sequentially across a wide range of energy loss to construct a 3-D dataset containing spatial and spectral information. For the analysis of sulfur, the energy width and the energy increment for the acquisition of energy-filtered images were set at 5 eV and at 3 eV, respectively. For zinc, the energy width was set at 10 eV and the energy increment was at 5 eV. EELS spectra from the regions of interest in an image can be synthesized by calculating the average gray values of the same pixels in each energy-filtered image over the whole range of acquired images. The image analysis system extracts the intensities at the same pixel in each image across the series, and reconstructs an EELS spectrum by plotting the intensities against the corresponding energy-loss values. The drift of the specimen was corrected by shifting the individual images pixelwise over the entire images acquired. Statistical digital image analysis was carried out using an image processing software, ANALYSIS (Soft Imaging Co. Ltd., Germany).

HAADF-STEM was performed with an HD2000 STEM (HITACHI Co. Ltd., Japan) operating at 200 kV equipped with a HAADF detector at a collecting angle ranging between 50 and 110 mrad and with a camera length of 1 cm.

## 3. Results and discussion

Fig. 1a and b shows a zero-loss image and an inelastically scattered image at 150 ± 10 eV energy losses by EFTEM, respectively, in a rubber matrix region. The zero-loss image (Fig. 1a) is formed with the electrons passing through the

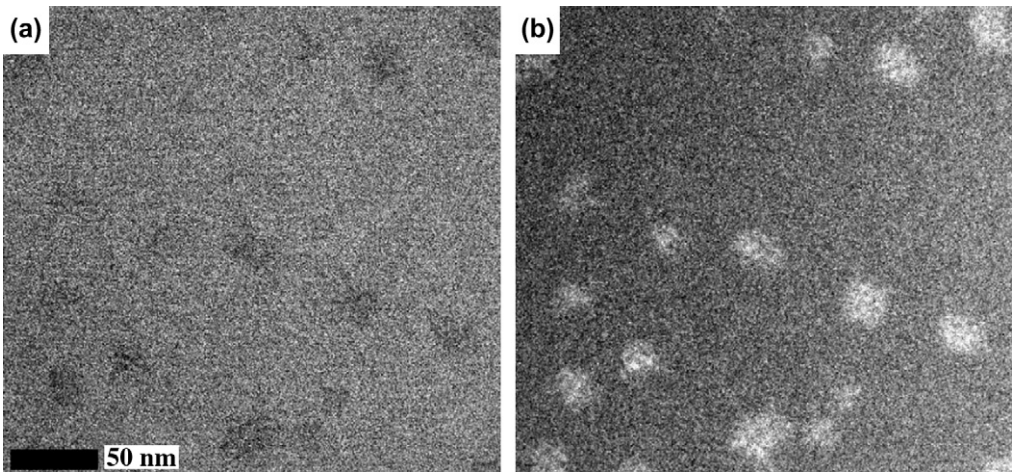


Fig. 1. (a) Zero-loss image; (b) energy-filtered image by EFTEM of matrix region of the accelerated vulcanized rubber.

specimen without the interaction (unscattered electrons) and with elastically scattered electrons, which is thus comparable with a conventional TEM image. The energy-loss image shown in Fig. 1b clearly exhibits the existence of numerous bright domains in the rubber matrix, whereas those are barely visible in the corresponding area of the zero-loss image shown in Fig. 1a. The average diameter and closest neighboring distance of about 200 particles were calculated and resulted in 20 and 37 nm with the standard deviation of 7.1 and 16.1 nm, respectively. Energy-loss images have frequently been helpful in visualizing structures that are hardly noticeable with conventional TEM. This convenient function of EFTEM is called as ''contrast tuning'', which can exhibit an image at an optimum condition by the tuning of the energy-loss levels [18–20]. All components in a specimen are presented with comparable contrast and intensity within the available gray levels. The energy-loss levels that provide an appropriate image contrast depend on specimen compositions and its specimen thickness. The optimum contrast of a specimen in which carbon is the majority element is usually achieved in a range from 100 to 250 eV, which is an energy-loss level below the carbon ionization K-edge at 285 eV.

Furthermore, we employed scanning transmission electron microscopy (STEM); it also gave images showing the distribution of the particles by introducing HAADF mode. Fig. 2a and b shows the bright field (BF) and the HAADF mode STEM images, respectively, demonstrating that the particles distributed in the rubber matrix can be observed in the HAADF mode (Fig. 2b). HAADF-STEM presents an image contrast that varies with atomic number ($Z$) by collecting elastically scattered electrons scattered at high angles. That is, high-$Z$ regions give brighter contrasts. Therefore, the particles distributed in the rubber matrix are suggested to be inorganic compounds containing high-$Z$ elements. As shown in Fig. 2c, HAADF-STEM can provide an image with a higher resolution than that by EFTEM, which allows us to know that the particles are not homogeneous products but rather are aggregates containing small products with about 3–5 nm in size. In order to investigate the elemental composition of the particles, energy-dispersive X-ray spectrometry (EDX) was performed using a convergent electron beam with a diameter of about 1 nm. Fig. 2d presents the EDX spectra acquired from the two regions inside and outside the particle indicated therein. The spectrum from the inside region shows both the zinc and sulfur peaks with the ratio of the integrated peak intensities (Zn/S) of approximately 1. On the other hand, in the region outside, only sulfur is detected and it appears with the weaker intensity, indicating that the sulfur detected in the rubber phase should be corresponding to the atoms involved in the rubber networks and zinc is almost absent in the rubber phase.

The EDX analysis suggests that the particles we found in the rubber matrix are mainly composed of ZnS. Studies on the mechanism of accelerated sulfur vulcanization by using low-molecular-weight model compounds revealed that ZnS is produced as a by-product [1,21,22], and also ZnS was experimentally detected in the study of mould fouling of rubber compounds [23]. Moreover, we detected ZnS localized in the interfacial region between rubber and ZnO particles added

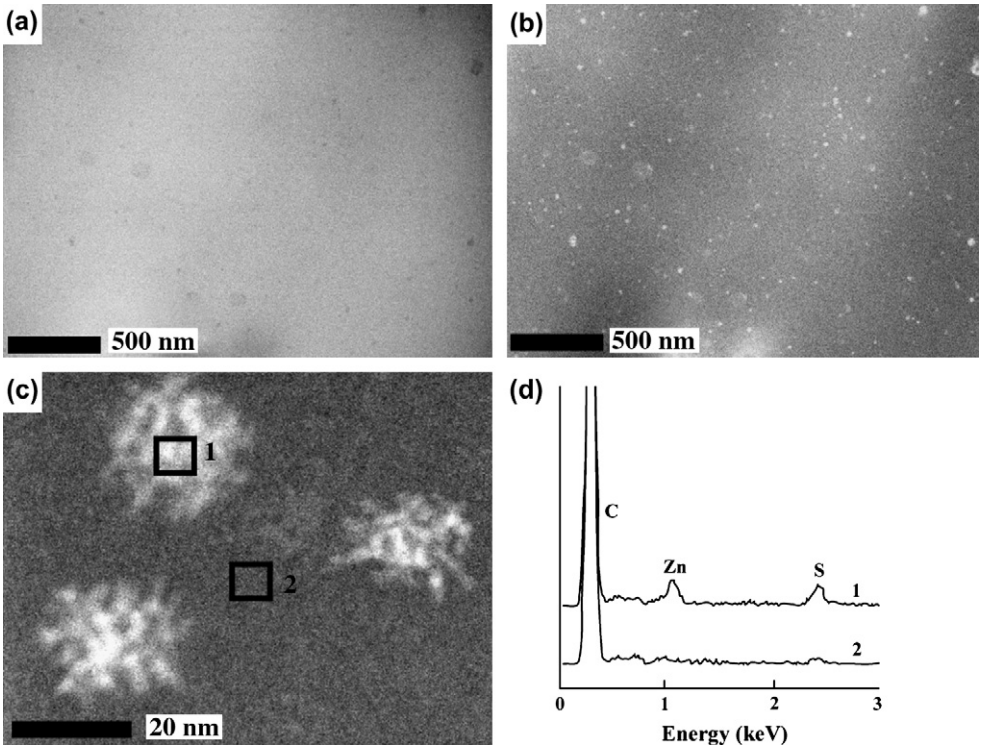


Fig. 2. (a) BF-STEM image; (b) HAADF-STEM image; (c) enlarged HAADF-STEM image shown in (b); (d) EDX spectra of the inside and outside of the particles shown in (c).

as an activator by EFTEM [18]. Further investigation here indicates that a large number of ZnS clusters are distributed over the entire area in the rubber phase as the form of the aggregation, which might largely influence the rubber network structures and the properties.

To obtain more detailed information on the structure of this product, EELS analysis was performed by Image-EELS technique that allows us to create EELS spectra from the regions of interest. We described the detailed procedure for creating elemental maps and EELS spectra by Image-EELS technique in our previous works [17,18]. Fig. 3a is a sulfur elemental map created by "two-window ratio" method, where the energy-filtered image beyond the ionization edge (core-loss image) of the element of interest was divided by the energy-filtered image below the edge (pre-edge image). In this case, the energy-filtered images at $140 \pm 10$ and $200 \pm 10$ eV were used as the pre-edge and the core-loss images, respectively, which were selected among the images acquired by Image-EELS. The sulfur elemental map shows that the domain is not a single homogeneous particle but rather is an aggregate of clusters. Fig. 3b and c shows sulfur-$L_{2,3}$ and zinc-$L_{2,3}$ ionization edges, which correspond to the L-shell excitation for the ionization of 2p electrons, after the background subtractions obtained from the three regions determined as depicted in Fig. 3a. The two regions within the domain, one of which is corresponding to the clusters (1) and the other of which is corresponding to the area between neighboring clusters (2), gave intense sulfur and zinc core-loss peaks, while the region outside of the domain (3: shown by blue) shows only sulfur ionization peak. The results thus obtained by EELS are in good agreement with the results obtained by EDX analysis by STEM.

EELS allows us to perform quantitative analysis in terms of the elemental compositions by using the integrated intensities of core-loss peaks, and furthermore, chemical shifts and shapes of EELS ionization edges can provide significant information on chemical structures in terms of coordinations, valencies and bond lengths [24]. We can, thus, obtain more detailed information from the EELS analysis in terms of the chemical structures of the sulfur and zinc-rich domains. The regions between the clusters in the domains, which appear darker than the clusters, gave both sulfur and zinc core-loss peaks with slightly weaker intensities than those obtained from the clusters. The integrated ratio with the energy width of 80 eV of the sulfur core-loss peak of the region 1 to that of region 2 is approximately 0.8, while the integrated ratio of the zinc core-loss peak with the width of 100 eV is 0.6. The concentrations of sulfur and zinc in region 2 are lower than those in region 1, and also the ratio of sulfur to zinc is slightly higher in region 2 than in region 1. Moreover, the

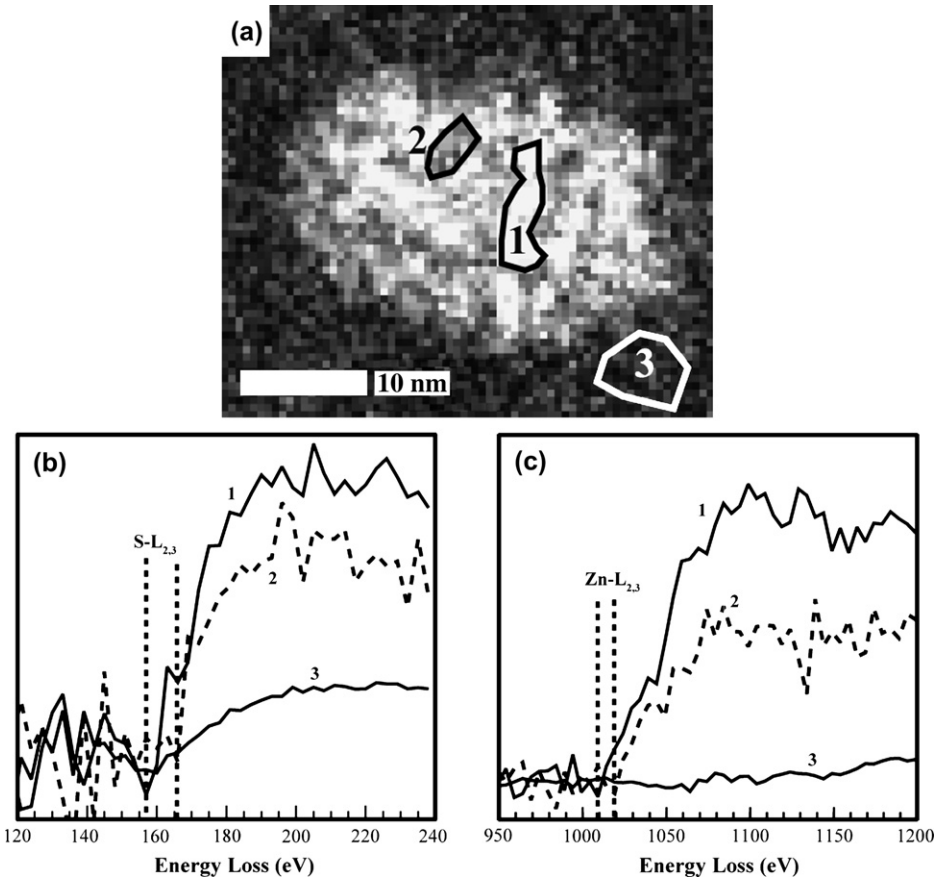


Fig. 3. (a) Sulfur elemental map obtained by EFTEM; (b) and (c) are the background-subtracted ionization edges of S-$L_{2,3}$ and Zn-$L_{2,3}$ in EELS spectra obtained from the regions indicated in (a), respectively.

spectra acquired from the two regions exhibit differences in terms of the energy-loss values at which the ionization events occur. That is, both the sulfur and zinc ionization edges obtained from region 2 appear at higher energy losses than in region 1, as shown in the spectra by dotted lines. The same results have been obtained in five different domains. These chemical shifts suggest the differences in the chemical bonds of the products between the two regions. These results suggest that the region between the clusters within the aggregate is not a simple rubber network, but rather it contains sulfur and zinc containing compounds differing from the ZnS cluster. Thus, the domains are not formed as a simple aggregation of the ZnS clusters, but are connected with each other via sulfur and zinc containing compounds that might be produced in the vulcanization process.

## 4. Conclusion

We here for the first time report on the formation of ZnS clusters in the vulcanized rubber matrix. Two sophisticated electron microscopic techniques revealed the heterogeneous character of the vulcanized rubbers that conventional TEM had identified as homogeneous. The fact that such a large number of small inorganic products are distributed throughout the rubber matrix requires in-depth study of the heterogeneity of rubber structures because elasticity and mobility of rubbers are significantly affected by such inorganic products and because large number of interfaces and inhomogeneous nano-sized structures are produced within the rubber networks. We will further investigate the effect of ZnS nanoparticles on the mechanical properties and also the effect of Acc types and vulcanization conditions on the formation of ZnS clusters.

## Acknowledgement

One of the authors (H.D.) gratefully thanks Prof. Tetsuo Asakura, Department of Biotechnology, Tokyo University of Agriculture and Technology, for his useful discussions with regard to this study. The authors also thank Y. Minagawa, H. Kishimoto, M. Sakai, H. Nakamae, H. Kimura and M. Kotani, SRI R&D, for their kind cooperation.

## References

[1] Heideman G, Datta RN, Noordermeer JWM, van Baale B. Rubber Chem Technol 2004;77:512–41.
[2] Labana SS, Newman S, Chompff AJ. In: Chompff AJ, Newman S, editors. Polymer networks, structure and properties. New York: Plenum Press; 1971. p. 453–75.
[3] Vilgis TA, Heinrich G. Kautsch Gummi Kunstst 1992;45:1006–14.
[4] Bastide J, Leibler L. Macromolecules 1988;21:2647–9.
[5] Vassilios G, Subramanian PR, Klein-Caster L. Macromol Symp 2001; 171:97–104.
[6] Alam TM, Cherry BR, Minard KR, Celina M. Macromolecules 2005;38: 10694–701.
[7] Harris DJ, Assink RA, Celina M. Macromolecules 2001;34:6695–700.
[8] Adriaensens P, Pollaris A, Vanderzande D, Gelan J, White JL, Kelchtermans M. Macromolecules 2000;33:7116–21.
[9] Veksli Z, Andreis M, Campbell DS. Polymer 1998;39:2083–8.
[10] Kwak SY, Kim SY. Polymer 1998;39:4099–105.
[11] Klei B, Koenig JK. Acta Polym 1997;48:199–207.
[12] Stein RS. J Polym Sci Part B Polym Lett 1969;7:657–60.
[13] Candau SJ, Bastide J, Delsanti M. Adv Polym Sci 1982;44:27–71.
[14] Reimer L, editor. Energy-filtering transmission electron microscopy. Heidelberg: Springer; 1995.
[15] Liu J. In: Wang ZL, editor. Characterization of nanophase materials. Weinheim: Wiley-VCH; 2000 [chapter 4].
[16] Benetatos NM, Smith BW, Heiney PA, Winey KI. Macromolecules 2005;38:9251–7.
[17] Horiuchi S, Yin D, Ougizawa T. Macromol Chem Phys 2005;206: 725–31.
[18] Horiuchi S, Dohi H. Langmuir 2006;22:4607–13.
[19] Horiuchi S, Hamanaka T, Aoki T, Miyanaka T, Narita R, Wakabayashi H. J Electron Microsc 2003;52:255–66.
[20] Horiuchi S, Matchariyakul N, Yase K, Kitano T, Choi HK, Lee YM. Polymer 1996;37:3065–78.
[21] Nieuwenhuizen PJ, Ehlers AW, Haasnoot JG, Janse SR, Reedijk J, Baerends EJ. J Am Chem Soc 1999;121:163–8.
[22] Geyser M, Mcgill WJ. J Appl Polym Sci 1996;60:431–7.
[23] Bukhina MF, Morozov YL, van de Ven PM, Noordermeer JWM. Kautsch Gummi Kunstst 2003;56:172–82.
[24] Braydson R. Electron energy loss spectroscopy. Oxford: BIOS Sci Pub; 2001 [chapters 5 and 6].